

# Longitudinal Beam Dynamics in Operation with Negative Momentum Compaction Factor on the UVSOR Electron Storage Ring

Masahito HOSAKA, Jun-Ichiro YAMAZAKI, Toshio KINOSHITA and Hiroyuki HAMA

UVSOR Facility, Institute for Molecular Science, Okazaki 444, Japan

To investigate variations of the bunch length and the energy spread of the electron beam on a storage ring, we have measured longitudinal electron distributions and spectra of spontaneous radiation from an optical klystron on the UVSOR storage ring operated with both signs of negative and positive momentum compaction factors. In general, the single bunch dynamic behavior such as lengthening of the bunched beam circulating in a storage ring is governed by the electromagnetic interaction between the impedance of the vacuum chamber. A longitudinal single bunch instability including increase of the energy spread of the beam due to high frequency impedance of many parts of the vacuum chamber, i.e., cavity, sudden change of pipes, groove, low Q cavity-like structure, etc., is well known as *microwave instability* [1]. On old machines, which were designed without deep consideration for the impedance, both longitudinal and transverse single bunch instability were often observed. However as far as recent reports on relatively new machines, there have been no clear evidence observed for the onset of microwave instability [2]. On the UVSOR ring, we have also observed no significant single bunch instability up to the maximum beam current can be stored at present. Based on a low Q resonator impedance model, Fang et. al. recently pointed out a possibility of which the threshold current for microwave instability would be high and the bunch lengthening would be not significant when a storage ring is operated with a negative momentum compaction factor [3].

In the nominal operation for users of synchrotron radiation (SR), a bit of a positive dispersion remains in straight sections to minimize the effective emittance, and then the momentum compaction factor  $\alpha$  is estimated to be + 0.035. For the experiment with negative  $\alpha$ , we developed a new operating point, where  $\alpha$  can be tuned smoothly from positive to negative without change of the betatron tunes. This operating point has been also optimized to use of the helical optical klystron with small gaps [4]. Calculated Twiss parameters of the lattice at positive and negative  $\alpha$  operations are shown in Fig. 1a and 1b, respectively.

A dual-sweep streak camera is a powerful tool to observe the electron distribution in the bunch and its variation in a certain time range [5]. Since a slow-sweep axis can be expanded up to 100 ms from the one turn period, we can not only observe the corrective longitudinal oscillation with the synchrotron frequency of about 15 kHz but also detect instabilities of which the electron distribution is slowly varied. Current dependent bunch lengthening has been measured up to  $\sim 100$  mA with the single-bunch mode for the almost same absolute values of the positive and the negative momentum compaction factors ( $|\alpha| = 0.033$ ). RMS bunch lengths were deduced from spectra averaged over many turns in the two-dimensional dual-sweep images of SR from a bending magnet. Figure 2 shows variations of the bunch length at a wide range of the single bunch current. For the case of the positive  $\alpha$ , the bunch lengthens monotonously, which is in

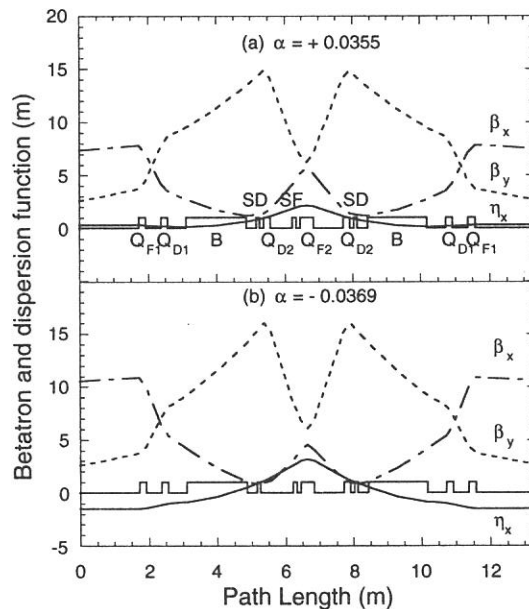


Fig.1 Calculated Twiss parameters for one unit cell at positive a (a) and negative a (b) operations.

agreement with our pervious measurements [6]. Based on potential-well distortion theory with a broad band impedance model [7], the bunch length  $\sigma_b$  at the average beam current  $I$  is expressed as

$$\left(\frac{\sigma_b}{\sigma_{b0}}\right)^3 - \left(\frac{\sigma_b}{\sigma_{b0}}\right) = \frac{e \alpha I [Z/n]_{eff}}{\sqrt{2} \pi v_s^2 E} \left(\frac{R}{\sigma_{b0}}\right)^3, \quad (1)$$

where  $\sigma_{b0}$  is the zero current (natural) bunch length and  $[Z/n]_{eff}$  is the effective longitudinal coupling impedance. By fitting the data for the positive  $\alpha$  with eq. (1), we obtained the effective impedance of 1.6  $\Omega$ , where we assumed no frequency dependence for  $[Z/n]_{eff}$ . As shown in Fig. 2, the fitting quality is not so bad that there seems to be no significant frequency dependence for  $[Z/n]_{eff}$  at the narrow region of which the bunch length observed.

Since the bunch lengthening due to potential-well distortion does not accompany increase of the energy spread, the *Keil-Schnell* criterion for the threshold condition of longitudinal microwave instability is able to be modified by replacing the peak current of the lengthened bunch [8].

The peak current for the Gaussian particle distribution is written as  $IC / (\sqrt{2} \pi \sigma_b)$ , the *Keil-Schnell* stability criterion is rewritten as

$$\sigma_b \geq \frac{C [Z/n]_{eff} I}{F \sqrt{2} \pi E |\alpha|} \left(\frac{\sigma_E}{E}\right)^{-2}, \quad (2)$$

where  $\sigma_E/E$  is the relative energy spread of the beam, respectively. A form factor of the particle distribution in the momentum space  $F$  is approximately the unity for bell-shape distributions. Using the deduced value of 1.6  $\Omega$  for  $[Z/n]_{eff}$ , a threshold bunch length for microwave instability estimated from eq. (2) is approximately 47 ps/mA. The beam with the bunch length below this line would be longitudinally unstable. However this threshold condition is obviously over estimated, because we have not observed clear evidence of instability even at the higher beam current of 100 mA with the positive  $\alpha$ . Since the *Keil-Schnell* stability criterion is for the worst case and the threshold condition should be varied by a combination of actual resistive and reactive impedances.

The bunch lengthening with the negative  $\alpha$  was drastically changed. As one can see, the bunch shortening was observed up to  $\sim 15$  mA, and then the bunch lengthened with the current. We confirmed the point of discontinuity around 15 mA as an onset of longitudinal microwave instability by the 2-dimensional streak camera image.

The bunch shortening can be simply explained assuming the wake field generated by an inductive ( $L$ ) impedance as  $V_{wake} = -L (dI/dt)$ . Since the synchronous phase of the beam with the negative  $\alpha$  is the opposite side of the slope of the accelerating RF field, a combined field with the RF field and the wake field becomes steep if the other is gently-sloping.

Radiation spectrum from the optical klystron is very sensitive to the beam energy spread. A modulation factor, which indicates degree of interference between two radiations from undulators separated by a dispersive section, defined as  $f_{mod} = (S_+ - S_-) / (S_+ + S_-)$ , where  $S_+$  and  $S_-$  are the maximum and the minimum intensities of a jagged-structure spectrum, respectively. Complete interference in both spatial and frequency domains makes  $f_{mod} = 1$ . An actual modulation factor may be separated into two terms as  $f_{mod} = f_\epsilon f_\gamma$  where  $f_\epsilon$  and  $f_\gamma$  are the modulation factors originated from the emittance and the energy spread, respectively. The analytical formula of  $f_\gamma$  is written as

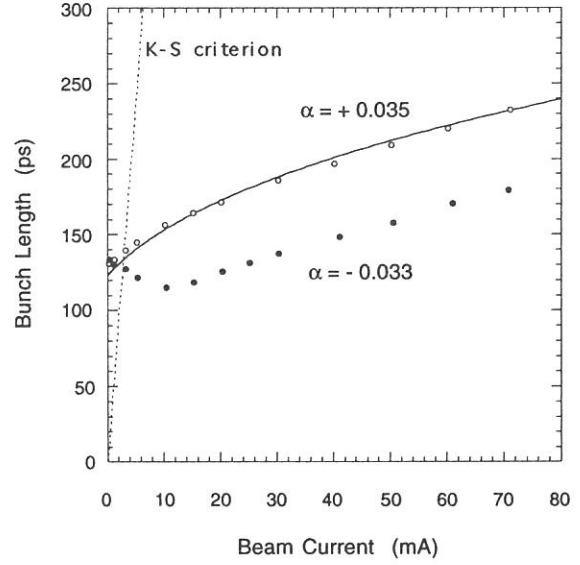


Fig. 2 Measured bunch lengths plotted as a function of the beam current.

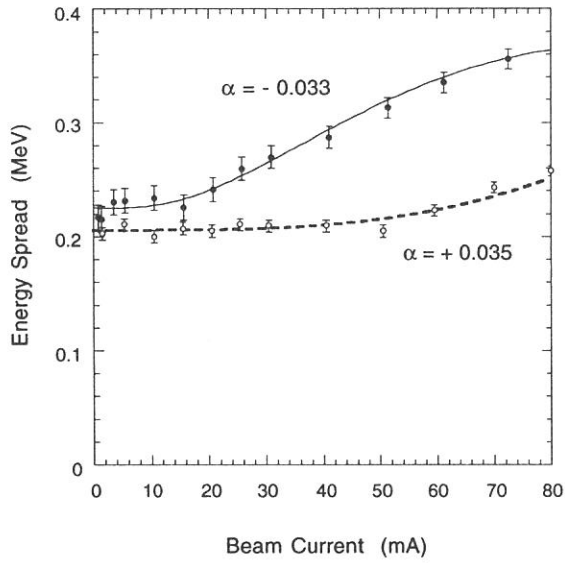


Fig. 3 Deduced energy spread from the modulation factor of the spontaneous spectra. Lines are drawn by eyes.

$$f_{\gamma} = \exp \left[ -8 \pi^2 (N_u + N_d)^2 \left( \frac{\sigma_E}{E} \right)^2 \right], \quad (3)$$

where  $N_u$  and  $N_d$  are the period number of one undulator and the interference order of the radiation.

We chose a resonant wavelength of 355 nm to measure the modulation factor, and  $N_d$  at the wavelength was 130. Results of the measurement of the energy spread are plotted as a function of the beam current in Fig. 3. One can apparently notice the threshold beam current around 15 mA exists for the increase of the energy spread in the negative  $\alpha$  operation, which corresponds with the result of the bunch length measurement. Meanwhile there seems to be no clear indication of the onset of microwave instability in the positive  $\alpha$  operation. Although there is a small discontinuity seen around the beam current of 50 mA, the increase rate of the energy spread at the higher beam current is slow. We have not identified whether microwave

instability occurred in the positive  $\alpha$  operation.

The normalized effective longitudinal impedance of  $1.6 \Omega$  was deduced from the bunch lengthening with the positive  $\alpha$ . The reason why the instability was occurred only in the negative  $\alpha$  operation is that the potential-well distortion due to the impedance acts to shorten the bunch length for the negative  $\alpha$  and the peak current reaches the threshold of instability at the lower beam current than the positive  $\alpha$ . The averaged bunch length with the negative  $\alpha$  is shorter than that with the positive  $\alpha$  at the wide range of the beam current. Nevertheless the negative  $\alpha$  operation has no advantage because of the lower threshold current of microwave instability. As far as the UVSOR ring, the suggestion of Fang et. al. is not realized. Probably the impedance model of a low Q resonator is not suitable for the UVSOR ring. As mentioned previously, the interaction between the electron bunch and the impedance of the chamber depends upon properties of the impedance, such as the combination of inductive and resistive components and the frequency dependence.

## References

- [1] for example; A. W. Chao, AIP Proc. No. 105 (American Institute of Physics, New York, 1983) 353.
- [2] A. H. Lumpkin et. al., Proc. 18th Int. Free Electron Lasers Conf., Rome, Italy, 1996.
- [3] S. X. Fang et. al., KEK Preprint 94-190 (National Laboratory for High Energy Physics, Tsukuba 1995).
- [4] H. Hama et. al., Proc. 3rd Aisan Symp. on Free Electron Laser (IONICS Publishing Co. Ltd., Tokyo 1997) 17.
- [5] H. Hama et. al., Nucl. Instr. and Meth. A375 (1996) 32.
- [6] H. Hama et. al., Proc. 9th Symp. on Accelerator Science and Technology, Japan (1993) 468.
- [7] B. Zotter, Proc. CERN Accelerator School, Paris 1984, CERN report 85-19 (CERN, Geneva, 1985) 415; J-L. Laclare, CERN Report 87-03 (CERN, Geneva, 1987) 264.
- [8] E. Keil and W. Schnell, CERN report ISR-TH-RF/69-48 (CERN, Geneva, 1969).

## A Question on Natural Chromaticity

Hiroyuki HAMA, Masahito HOSAKA, Jun-Ichiro YAMAZAKI, Toshio KINOSHITA

*UVSOR Facility, Institute for Molecular Science, Okazaki 444, Japan*

Chromaticity represents strength of momentum dependence of the betatron tune in circular accelerators. Natural chromaticity of a separated function storage ring is normally negative, so that the chromaticity is corrected to be zero or slightly positive by using sextupole fields to avoid a head-tail instability because a momentum compaction factor is usually positive. Since there are two families of sextupole magnets on the UVSOR ring, the corrected chromaticity  $\xi$  is written in a frame of the linear lattice function as

$$\xi = a SF + b SD + \xi_0, \quad (1)$$

where  $SF$  and  $SD$  are strengths of each sextupole family, and  $a$ ,  $b$  and  $\xi_0$  are coefficients depend on the lattice functions and the natural chromaticity, respectively. The chromaticity is able to be experimentally deduced from the tune shift caused by change of the electron momentum. If one obtain a series of chromaticities as a function of strengths of  $SF$  and  $SD$ , the natural chromaticity can be deduced. In operations with negative momentum compaction factors, the beam is not killed with no sextupole fields, so that the natural chromaticity can be directly obtained.

We have measured the natural chromaticities for various operating points, and the experimental ones were compared with the calculated ones. Representative operating points in the experiments are  $(v_x, v_y) = (3.16, 2.64)$  and  $(3.16, 1.44)$ , and the momentum compaction factor was varied from + 0.03 to - 0.03 on each operating point. Although the coefficients  $a$  and  $b$  strongly depend on magnitudes of the beta functions at positions of the sextupoles, it is usually very difficult to change the Twiss parameter so much. According to the calculations, the natural chromaticity was able to be varied from - 3 to - 6 and from - 4.5 to - 6.5 in the horizontal and the vertical planes, respectively. Experimental results are shown in Fig. 1. For the horizontal chromaticity, a good agreement with the calculation can be seen. However a big discrepancy is obvious for the vertical chromaticity.

It is easily imagined that some additional multipole field exists in the ring. Since the horizontal beta function is relatively lower than the vertical beta function around the bending magnets to reduce the emittance in the Chasman-Green lattice, we have assumed a sextupole field is created in the fringe of the bending magnets. By using a thin lens approximation, an identical additional sextupole is added to both edges of the bend and its strength was estimated to reproduce the experimental data. Because there was no solution to simultaneously reproduce both the horizontal and the vertical experimental data, we obtained the strength of additional sextupole independently for each direction and each data, and averaged it. Consequently we

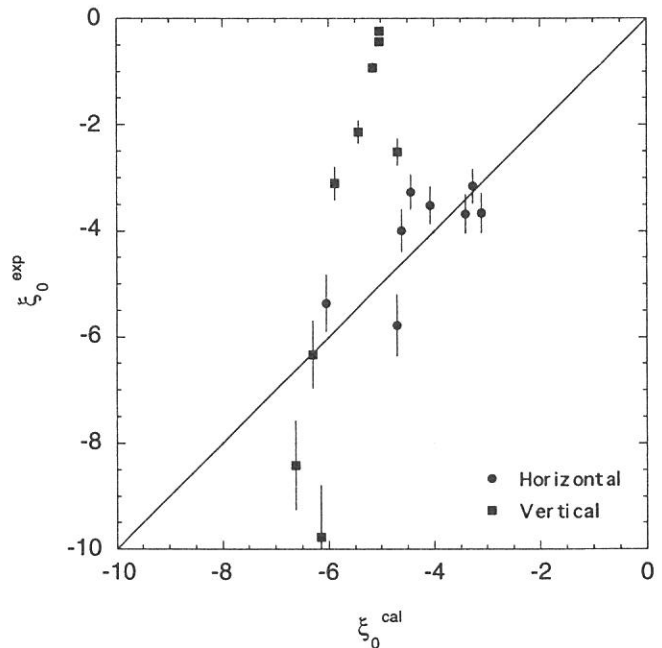


Fig.1 Measured natural chromaticities plotted as a function of the calculated ones.

obtained a strength  $+ 1.43 (\pm 0.40) T/m^2 m$  for a beam rigidity of  $2 T m$  ( $E = 600 \text{ MeV}$ ). This magnitude of the additional sextupole is unexpectedly strong. Note the strength of the sextupoles is usually  $\sim 8 T/m^2 m$  in the normal operation.

Because we have made the sextupole strength represents the whole additional multipole field in the bend, this is probably not perfectly correct. However the most of experimental data is able to be reasonably reproduced as shown in Fig. 2. Unfortunately there was no precise information on the fringe field of the bending magnet, it is difficult to discuss qualitatively whether the additional sextupole is a proper model. In another experiment, we have measured higher order dispersion functions. Because those quantities are much affected by the sextupole field, this additional field will be examined.

Anyhow the chromaticity has been practically estimated well by adding the fringe sextupole field in the linear lattice calculation. The strength of the regular sextupole magnets can be, therefore, calibrated by the calculations. We have used identical magnets and power supplies for the sextupole families. The strengths of the sextupole families have been calculated to reproduce the experimental chromaticity at each operating point and excitation current. Since the strength of the sextupole field is proportional to the excitation current, we would obtain an empirical relation between the field strength and the excitation current.

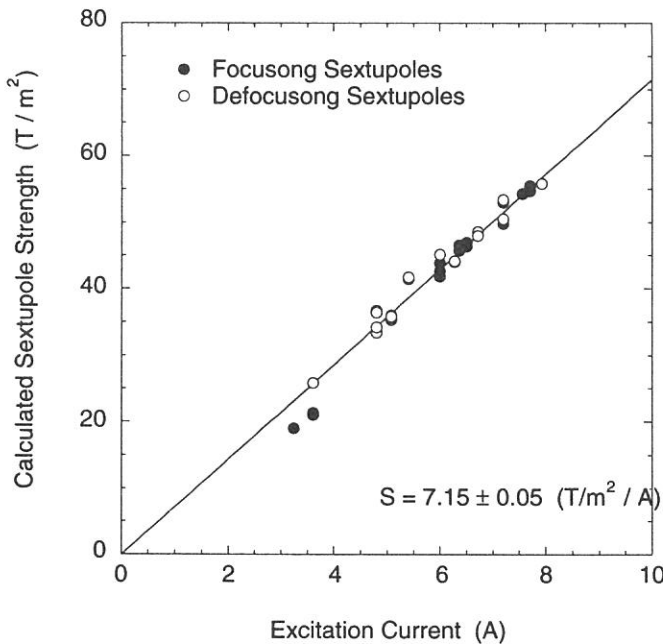


Fig. 3 Calculated field strengths of sextupoles plotted as a function of the excitation current.

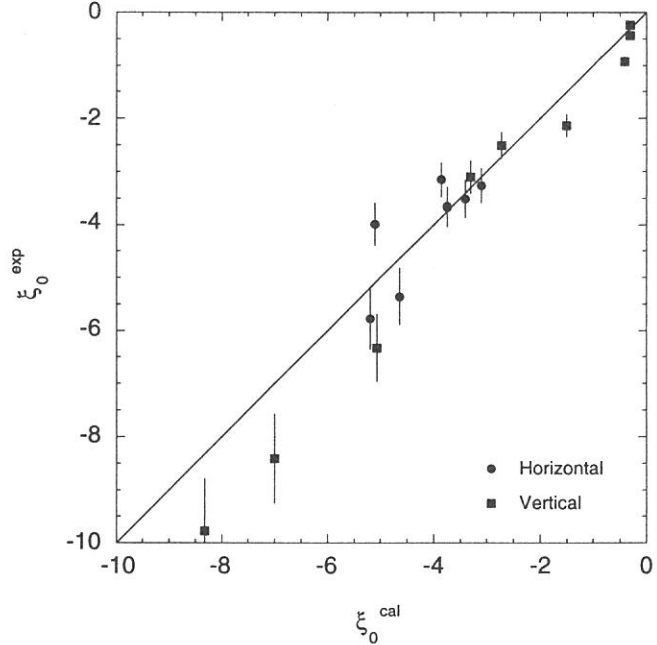
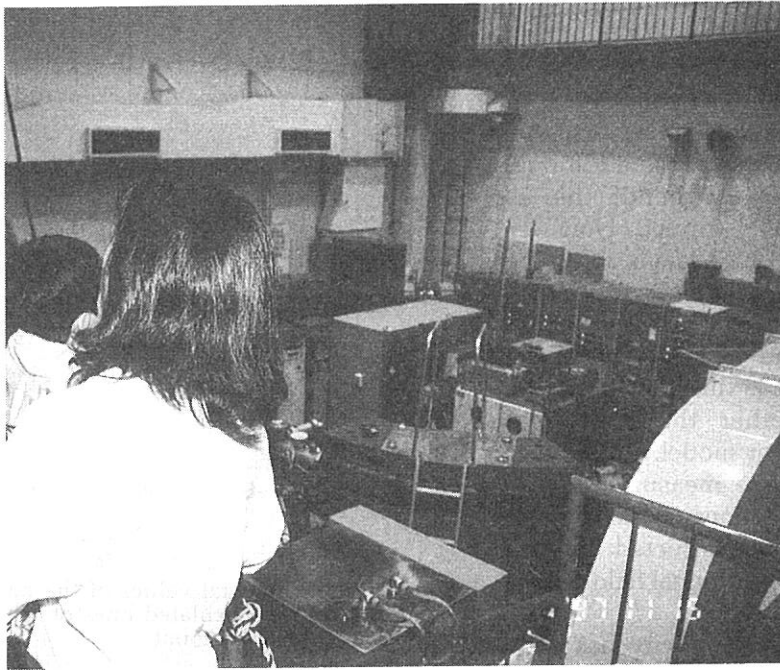


Fig. 2 The experimental values of the natural chromaticity compared with the calculated ones of which the additional sextupole is taken into account.

The result is shown in Fig. 3. As one can see, the linearity of the strength is fairly good, and a strength parameter of  $7.15 T/m^2/A$  was obtained. Unfortunately we have no measured data of the sextupole magnets. The design value of the field strength parameter is  $6.7 T/m^2/A$ , which is not far from the result.

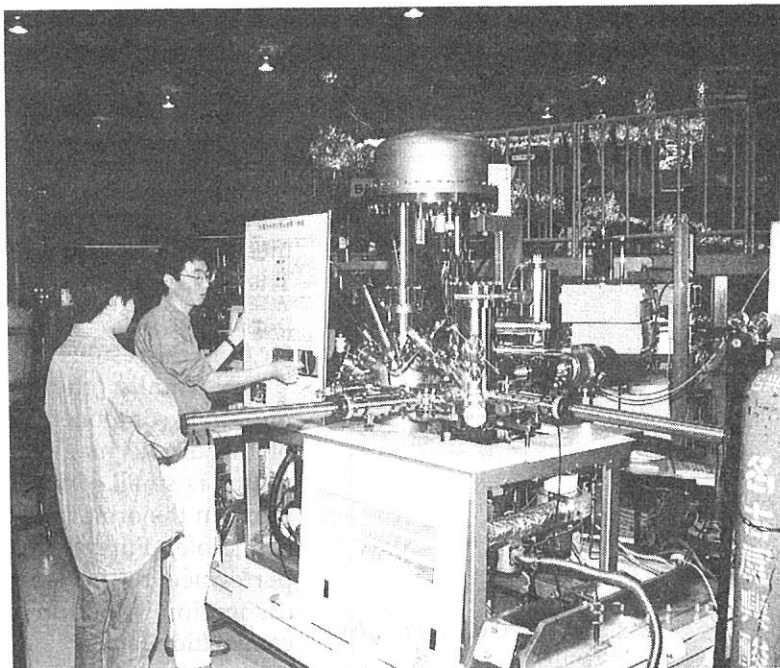
Normally there are complicate multipole components exist in the fringe of the dipole magnets whose bending radius is small. In this case the kinetic terms in the orbit calculation may be not negligible. Further investigation will be performed by measuring higher order dispersion function and momentum compaction factor.





“Mum, how the electron is accelerated at the synchrotron?”

*“Open House” on Nov. 15*



“OK. Let me tell you what is interesting of the photoelectron microscopy.”

*“Open House” on Nov. 15*